Scanning Kelvin-probe study of the hydrogen-terminated diamond surface in ultrahigh vacuum

C. I. Pakes,[1,a)] D. Hoxley,[1] J. R. Rabeau,[2] M. T. Edmonds,[1] R. Kalish,[3] and S. Prawer[4]
[1]*Department of Physics, La Trobe University, Victoria 3086, Australia*
[2]*Department of Physics, Macquarie University, New South Wales 2109, Australia*
[3]*Department of Physics and Solid State Institute, Technion, Haifa 32000, Israel*
[4]*Centre for Quantum Computer Technology, School of Physics, University of Melbourne, Victoria 3010, Australia*

(Received 2 April 2009; accepted 17 August 2009; published online 23 September 2009)

Atomic-force and Kelvin-probe microscopies were employed in ultrahigh vacuum to image the surface topography and contact potential of the hydrogen-terminated and unterminated surfaces of diamond. A variation of about 25 meV in the contact potential was measured on a length scale of 20 nm and ascribed to differently orientated surface domains resulting from hydrogen-plasma processing of the sample. Shifts in the work function arising from sample heating in vacuum and the adsorption of C_{60} were measured. The Fermi level was found to be 0.7 and 1.1 eV below the valence band maximum for C_{60} coverages of 1 and 4 monolayer, respectively. © *2009 American Institute of Physics*. [doi:10.1063/1.3222864]

The electronic properties of the diamond surface continue to exhibit interesting phenomena, with potential for application to nanoelectronics. While the free surface of diamond is insulating, hydrogen termination of the surface provides a mechanism by which subsequently adsorbed molecular species may act as acceptors, giving rise to *p*-type accumulation of the underlying surface via surface transfer doping.[1] Atmosphere-induced surface conductivity has been studied in detail using photoemission techniques,[2,3] probe microscopy,[4] and transport measurements,[5] which indicate low carrier concentrations and evidence of disorder. Furthermore, studies based upon different techniques and samples have given contradictory information, such as in the position of the Fermi level in the presence of doping.[4,6] The use of synthetic acceptors, C_{60} and $C_{60}F_{48}$, to induce subsurface hole accumulation has recently been demonstrated by surface transport measurements,[6,7] and may be an important step toward the development of quantum electronic devices utilizing hole transport at the diamond surface. To this aim it is necessary to fully understand the effect on the surface electronic properties of the introduction of molecular surface acceptors. However, with the exception of transport measurements,[6,7] no experimental studies have been performed to monitor surface band bending as the surface is doped with fullerene.

Scanning Kelvin-probe microscopy (SKM) is well suited to this problem since knowledge of how the work function shifts in response to surface doping reflects the extent of band bending and variation of the Fermi level. The Fermi energy, relative to the valence band maximum, is related to the surface work function, ϕ, the bandgap, E_g, and the electron affinity, χ, according to $E_F = E_g + \chi - \phi$. SKM has been applied in air to measure the work function of hydrogen-terminated diamond surfaces.[4] However, exposure to ambient conditions has important adverse consequences. In the SKM technique, measurement of the contact potential difference (CPD) between the probe and hydrogen-terminated diamond surface will be influenced by an adsorbed water layer and other airborne contaminants, which make ambient SKM techniques unreliable. Furthermore, an adsorbed water layer significantly effects the surface electron affinity,[8] which has an accepted value of about -1.3 eV in vacuum for the hydrogen-terminated C(100) surface,[2] but may be as low as -0.5 eV for a surface in contact with water.[9] This makes evaluation of the Fermi level from an ambient measurement of work function unreliable. Most importantly, for the study of synthetic surface acceptors, ambient SKM measurements cannot differentiate between the effects on the work function of water-based surface acceptors and deliberately introduced synthetic acceptor molecules. A measurement of the response of the work function to fullerene doping therefore necessitates the application of SKM techniques in vacuum. This paper reports ultrahigh vacuum (UHV) atomic-force and Kelvin-probe imaging of the diamond surface. SKM is applied in UHV to monitor the response of the surface to sample heating, which removes water-based adsorbates, and to the deposition of C_{60}.

Two different diamond substrates have been considered. Both were boron doped, introducing a bulk conductivity to eliminate the effects of sample charging during SKM measurements. In this manner, the application of UHV-SKM provides reliable measurement of the work function even in the absence of a hydrogen-termination, and may be used to determine shifts in the Fermi energy to low acceptor coverages, which are known to induce very low levels of surface conductivity.[6] Measurement of the response of the work function of hydrogenated and unhydrogenated surfaces to thermal annealing were performed on a boron-doped polycrystalline diamond film, with a resistivity 0.1 Ω cm (sample I). Experiments measuring the response of the surface to deliberate doping with C_{60} used a type-IIa (100) single crystal diamond which had been deliberately doped to a resistivity of 2×10^{-3} Ω cm by boron-ion implantation (sample II). Samples were cleaned by boiling in acid ($H_2SO_4/HCLO_4/HNO_3$; 1:1:1). Unhydrogenated (nominally oxygen terminated) surfaces were prepared by expos-

a)Electronic mail: c.pakes@latrobe.edu.au.

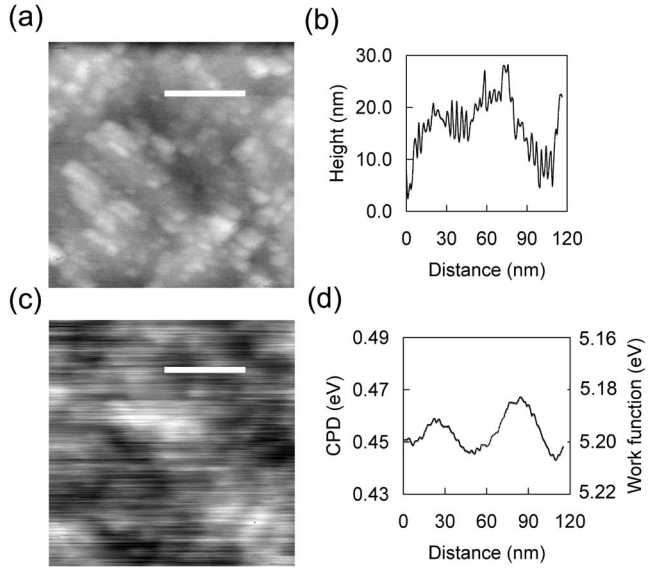

FIG. 1. Noncontact AFM (a) and Kelvin-probe (c) images obtained for the same area of the polycrystalline sample (sample I), immediately after insertion into UHV; the scan size is 350 nm × 350 nm in each case. [(b) and (d)] show scans of surface topography and CPD along the lines indicated in the corresponding images.

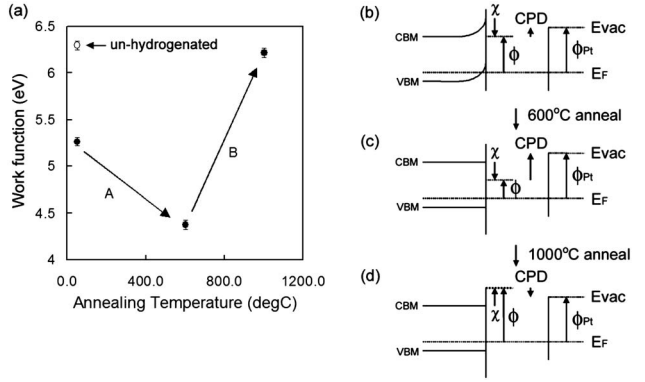

FIG. 2. (a) Measured work function of virgin and annealed hydrogenated surfaces (●) and unhydrogenated surface (○) for sample I. Anneal A: 600 °C; anneal B: 1000 °C. [(b)–(d)] Schematic representation (not to scale) of the band-edge diagram at the hydrogenated diamond surface, relative to the probe: (b) virgin H-terminated film exposed to atmosphere; (c) H-terminated film following 600 °C anneal; (d) H-desorbed film following 1000 °C anneal.

ing the acid-etched samples to ambient conditions. Hydrogen termination of the samples was performed by plasma treatment in a 30 Torr 1.2 kW microwave hydrogen plasma. The sample temperature was gradually decreased from 800 to 400 °C during the course of the termination, which totalled 50 min. All surfaces were exposed to air before being transferred to UHV (10^{-10} mbar). Sample heating in UHV was achieved by fixing the diamond samples using Ta clamps to an underlying Si sample that could be heated via a direct current; the temperature of the underlying Si was monitored during *in situ* heating and used as a measure of the diamond sample temperature. C_{60} deposition was performed by sublimation from a Knusden cell; the pressure in the vacuum system reached 10^{-8} mbar during operation of the evaporator. SKM measurements were performed after each evaporation step of C_{60}.

Kelvin-probe measurements were performed at room temperature using a JEOL 4500 atomic force microscope (AFM), fitted with Pt-coated Si cantilevers, with a force constant of 11.5 N m^{-1}. The force gradient between the probe and surface was detected using a phase-locked loop (PLL) to monitor and maintain a shift in the resonant frequency of the cantilever. By applying an alternating bias, of amplitude 1 V at 1 kHz, to the cantilever and monitoring the PLL output at this frequency using a lock-in amplifier, the addition of a dc bias, as a feedback signal, yields the CPD between surface and probe when the PLL response vanishes.[10,11] The work function, ϕ, is then obtained with respect to the work function of the Pt-coated probe, ϕ_{Pt}, according to $\phi=\phi_{Pt}-\mathrm{CPD}$, where $\phi_{Pt}=5.65$ eV.[12]

Figure 1 illustrates atomic-force and CPD images of the H-terminated surface for sample I after insertion into UHV. The AFM revealed topographic features on the scale of about 20 nm. Features could be observed also in the CPD image on this length scale, with variation of about 25 meV in the local CPD. It is known that hydrogen-plasma exposure of the diamond surface at a temperature in the range of 400–800 °C can lead to an increased surface roughness on this scale,[13] arising from the formation of {111}-orientated facets during anisotropic etching of the surface.[14] The electronic properties of the hydrogen-terminated surface depend upon its orientation. The electron affinity of the H-terminated C(111) surface is 30 meV lower than that of the C(100) surface, due to a higher surface dipole density for C(111) compared to C(100).[2,3] While the grains of a polycrystalline diamond sample are in principle large (tens of microns), hydrogen-plasma etching will give rise to the formation of differently orientated facets. Since neighboring facets share a common Fermi level, spatial variation in the local work function or CPD will reflect variation of the electron affinity. The measured spatial variation in the CPD is consistent with the difference in electron affinity between the hydrogen-terminated C(100) and C(111) surfaces.[2,3] The observed roughness both in topography and local CPD can therefore be attributed to facet formation during hydrogen-plasma processing.

To determine the response of the work function to changes in surface state (sample I) a spatially averaged CPD was determined for each image, based upon the measured CPD averaged over repeated 300 nm × 300 nm images. Immediately after insertion into UHV, the hydrogen-terminated surface was found to have a work function of 5.3 ± 0.1 eV, while the unterminated surface yielded a work function of 6.3 ± 0.1 eV. Figure 2(a) indicates the work function of the as-prepared surfaces for sample I and illustrates the response of the hydrogen-terminated surface to annealing in UHV. Heating the H-terminated surface to 350 °C for 10 min followed by 600 °C for 10 min (anneal A), decreases the work function to 4.4 ± 0.1 eV. A subsequent anneal at 600 °C overnight, followed by 1000 °C for 60 min (anneal B), increases the work function by 2 eV to a value similar to that of the unterminated surface. The response to heating in UHV is consistent with extensive macroscopic studies of the electron affinity and work function of hydrogenated diamond surfaces,[2,3] confirming the accuracy of the SKM measurements. The response of the surface to heating is illustrated schematically as a series of band diagrams in Figs. 2(b)–2(d). Heating to 600 °C gives rise to the desorption of surface acceptors, resulting in removal of the subsurface hole accumulation layer, in addition to hydrocarbon contaminants.[2] The observed decrease in work function indicates an increase of 0.9 eV in the Fermi level. Heating to

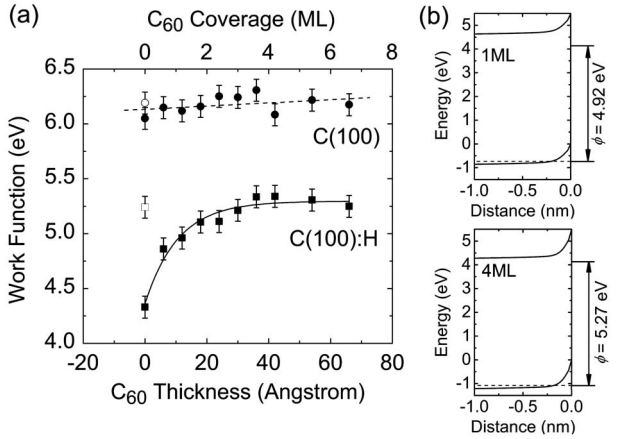

FIG. 3. (a) Measured work function of hydrogenated and unhydrogenated C(100) surface for sample II. Open symbols: samples immediately after insertion into UHV. Closed symbols indicate the effect of fullerene film deposition, following heating to 600 °C. The solid line is a fit of the form $\phi(\mathrm{eV})=\phi_0-\phi_1\exp(-t/\alpha)$; the broken line is a linear fit to the data for the unterminated surface. (b) Numerical band diagrams corresponding to C_{60} coverages of 1 and 4 ML.

1000 °C causes desorption of hydrogen from the surface; the observed increase in work function is then consistent with an increase in electron affinity to a positive value.

The response of the hydrogen-terminated and unterminated diamond surfaces to surface doping with C_{60} was measured using sample II. Work function measurements for both surface states as a function of C_{60} coverage are illustrated in Fig. 3(a); data for the as-prepared surfaces are represented by the open symbols. To identify changes in the work function due to fullerene doping, the effects of surface charge transfer arising from exposure to ambient conditions were first eliminated by heating the surfaces to 600 °C (anneal A). Upon heating, a significant drop in work function was observed for the hydrogen-terminated surface only, to a value of 4.3 ± 0.1 eV, consistent with the behavior of sample I. The solid symbols in Fig. 3(a) illustrate the response to subsequent C_{60} doping. The work function of the unhydrogenated surface remains unchanged. For the hydrogen-terminated surface, the work function increases, recovering to an as-prepared level of 5.3 ± 0.1 eV following deposition of a C_{60} film of thickness 40 Å. To verify that the observed behavior was not a consequence of the increase in pressure in the vacuum chamber during fullerene sublimation, the experiment was repeated with freshly prepared samples without exposing the surface to the C_{60} flux during operation of the evaporator. No change in work function was observed in this case. In addition, Raman spectroscopy was used to show that during deposition the C_{60} did not dissociate. The increase in work function monitored for the hydrogen-terminated sample is therefore a consequence of surface doping following the adsorption of C_{60}. The evolution of the work function with C_{60} film thickness, t, was fitted to an equation of the form $\phi(\mathrm{eV})=\phi_0-\phi_1\exp(-t/\alpha)$, where $\phi_0=5.30\pm0.04$ eV and $\phi_1=0.93\pm0.07$ eV, yielding the solid curve in Fig. 3. The fitting parameter $\alpha=1.1\pm0.2$ nm is consistent with the diameter of a single C_{60} molecule, so that the term t/α therefore represents the fullerene surface coverage. A rapid increase in work function, of 0.7 eV, was observed during adsorption of the first monolayer of C_{60}. The observed saturation in the work function of the hydrogen-terminated surface following adsorption of C_{60} to a surface coverage of about four monolayers is consistent with the saturation in induced surface conductivity observed in transport measurements,[6] pointing towards the need to form a solid film of C_{60} for efficient surface doping to take place. Figure 3(b) shows numerical band diagrams illustrating the band bending arising from C_{60} coverages of 1 and 4 ML. The potential profile in each case has been derived from a self-consistent solution of the Poisson and Schrödinger equations using the Fermi energy as a variable parameter.[15] The Fermi level was determined from the work function measurement for the corresponding surface coverage, taking into account a negative electron affinity in vacuum of −1.3 eV. The Fermi level is 0.7 eV below the valence band maximum for 1 ML coverage and 1.1 eV below the valence band maximum for 4 ML coverage of C_{60}.

In summary, UHV Kelvin-probe microscopy has been used to image the surface topography and CPD of the hydrogen-terminated diamond surface. A spatial variation of about 25 meV in CPD was observed on a 20 nm length scale, ascribed to variation in surface orientation due to anisotropic plasma etching. Sample heating in UHV and the adsorption of fullerene give rise to large, reproducible changes in the work function that may be accurately measured using this technique. The variation in work function, as a function of C_{60} coverage has been determined.

We acknowledge financial support of the Australian Research Council.

[1] F. Maier, M. Riedel, B. Mantel, J. Ristein, and L. Ley, Phys. Rev. Lett. **85**, 3472 (2000).
[2] F. Maier, J. Ristein, and L. Ley, Phys. Rev. B **64**, 165411 (2001).
[3] J. B. Cui, J. Ristein, and L. Ley, Phys. Rev. Lett. **81**, 429 (1998).
[4] B. Rezek, C. Sauerer, C. E. Nebel, M. Stutzmann, J. Ristein, L. Ley, E. Snidero, and P. Bergonzo, Appl. Phys. Lett. **82**, 2266 (2003).
[5] C. E. Nebel, B. Rezek, and A. Zrenner, Phys. Status Solidi A **201**, 2432 (2004).
[6] P. Strobel, M. Riedel, J. Ristein, and L. Ley, Nature (London) **430**, 439 (2004).
[7] P. Strobel, M. Riedel, J. Ristein, L. Ley, and O. Boltalina, Diamond Relat. Mater. **14**, 451 (2005).
[8] G. Piantanida, A. Breskin, R. Chechik, O. Katz, A. Laikhtman, A. Hoffman, and C. Coluzza, J. Appl. Phys. **89**, 8259 (2001).
[9] J. Ristein, W. Zhang, and L. Ley, Phys. Rev. E **78**, 041602 (2008).
[10] C. I. Pakes, D. Hoxley, S. Rubanov, J. R. Rabeau, S. M. Hearne, D. N. Jamieson, S. Prawer, and R. Kalish, Surf. Sci. **601**, 5732 (2007).
[11] S. Kitamura and M. Iwatsuki, Appl. Phys. Lett. **72**, 3154 (1998).
[12] D. E. Eastman, Phys. Rev. B **2**, 1 (1970).
[13] R. E. Stallcup and J. M. Perez, Phys. Rev. Lett. **86**, 3368 (2001).
[14] C.-L. Cheng, H.-C. Chang, J.-C. Lin, K.-J. Song, and J.-K. Wang, Phys. Rev. Lett. **78**, 3713 (1997).
[15] M. T. Edmonds, C. I. Pakes, and L. Ley, "A self-consistent solution of the Schrodinger-Poisson equations for hydrogen terminated diamond," Phys. Rev. B (submitted).